Keratinocyte desmosomal cadherin Desmoglein 1 as a mediator and target of paracrine signaling in the melanoma niche

Hope E. Burks [1], Jenny L. Pokorny [1], Jennifer L. Koetsier [1], Quinn R. Roth-Carter [1], Christopher R. Arnette [1], Pedram Gerami [1,2,3], John T. Seykora [4], Jodi L. Johnson [1,2], Kathleen J. Green [1,2,3]

[1]Department of Pathology, Feinberg School of Medicine, Northwestern University, Chicago, Illinois.

[2]Department of Dermatology, Feinberg School of Medicine, Northwestern University, Chicago, Illinois.

[3]Robert H. Lurie Comprehensive Cancer Center, Northwestern University, Chicago, Illinois.

[4]Department of Dermatology, Perelman School of Medicine at the University of Pennsylvania, Philadelphia, Pennsylvania.

Corresponding Author:

Kathleen J. Green, Ph.D.

Department of Pathology

Northwestern University

Feinberg School of Medicine

303 E Chicago Ave., Chicago, IL 60611

Telephone: 312-503-5300

Email: kgreen@northwestern.edu

Abstract

Melanoma is an aggressive cancer typically arising from transformation of melanocytes residing in the basal layer of the epidermis, where they are in direct contact with surrounding keratinocytes. The role of keratinocytes in shaping the melanoma tumor microenvironment remains understudied. We previously showed that temporary loss of the keratinocyte-specific cadherin, Desmoglein 1 (Dsg1) controls paracrine signaling between normal melanocytes and keratinocytes to stimulate the protective tanning response. Here, we provide evidence that melanoma cells hijack this intercellular communication by secreting factors that keep Dsg1 expression low in surrounding keratinocytes, which in turn generate their own paracrine signals that enhance melanoma spread through CXCL1/CXCR2 signaling. Evidence suggests a model whereby paracrine signaling from melanoma cells increases levels of the transcriptional repressor *Snai2* (Slug), and consequently decreases the Dsg1 transcriptional activator *Grhl1* (Grainyhead like 1), a known promoter of epidermal differentiation and barrier function. Together, these data support the idea that paracrine crosstalk between melanoma cells and keratinocytes resulting in chronic keratinocyte Dsg1 reduction contributes to melanoma cell movement associated with tumor progression.

Introduction

Cutaneous melanoma is a deadly skin cancer arising from pigmented melanocytes within the epidermis. Interactions between melanoma cells and their surrounding microenvironment play a critical role in tumor initiation and progression (Brandner and Haass, 2013; Villanueva and Herlyn, 2008; Wang et al., 2016). Discoveries surrounding immune cell interactions in solid tumors have led to significant innovation in clinical treatment strategies across multiple malignancies including melanoma (Kalaora et al., 2022). Similarly, the role of fibroblast-melanoma cell interactions has been integral to understanding melanoma spread within the dermis (Galbo et al., 2021). However, less is known about how communication between melanocytes and their more

51 abundant keratinocyte neighbors promotes melanoma development or initial stages of melanoma
52 movement within and away from the epidermal environment.

53 It is well known that melanocyte-keratinocyte communication is crucial for mediating
54 protective responses to ultraviolet radiation (UV) (Upadhyay et al., 2021; Wang et al., 2016;
55 Yardman-Frank and Fisher, 2021). UV elicits a cascade of signaling between the two cell types,
56 resulting in the production of melanin by melanocytes, which is transferred to keratinocytes, where
57 the pigment is positioned over the nucleus to protect DNA from UV-mediated damage. Changes
58 in communication between pigmented cells and keratinocytes continuously evolve in the
59 developing melanoma environment (Brandner and Haass, 2013). Melanoma cells can escape
60 control by adjacent keratinocytes by losing their intercellular contacts, allowing uncontrolled
61 proliferation and spread (Wang et al., 2016). Cell contact between radially spreading melanoma
62 cells and differentiated keratinocytes can then trigger vertical growth through Notch signaling,
63 promoting movement of melanoma cells into the dermis (Golan et al., 2015). Major contributors
64 to cell contact-mediated communication between keratinocytes and melanocytes are members of
65 the cadherin family of cell-cell adhesion molecules. For instance, loss of E-cadherin (Ecad) is
66 associated with the loss of keratinocyte control over melanoma cell proliferation and invasion
67 (Haass et al., 2005; Hsu et al., 2000). Further, increased P-cadherin stabilizes heterotypic
68 adhesions between keratinocytes and melanoma cells to promote melanoma cell expansion and
69 is associated with reduced survival in humans (Mescher et al., 2017).

70 Beyond cadherins' functions in direct contact, a role for vertebrate-specific cadherins
71 known as desmogleins in paracrine signaling has recently emerged. Desmogleins work with
72 partner desmocollin proteins to make up the adhesive core of desmosomes, essential intercellular
73 junctions that provide structural integrity to the skin and are critical for epidermal barrier function
74 (Hegazy et al., 2022; Kowalczyk and Green, 2013). Desmoglein 1 (Dsg1) is a keratinocyte specific
75 desmosomal cadherin found in complex stratified tissues of terrestrial organisms (Green et al.,

76 2020). Work in our lab has shown that Dsg1 plays roles in cell signaling independent of its role
77 as an adhesion molecule. Dsg1 promotes keratinocyte differentiation through suppression of
78 EGFR-MAPK signaling by associating with Erbin, ultimately inhibiting Ras-Raf complex formation
79 upstream of ERK1/2 to promote differentiation (Harmon et al., 2013). Dsg1 also controls cytokine
80 signaling to dampen inflammation, and its loss in patients with bi-allelic mutations in Dsg1 results
81 in the inflammatory condition severe dermatitis, multiple allergies and metabolic wasting (SAM)
82 syndrome (Godsel et al., 2022; Polivka et al., 2018; Samuelov et al., 2013).

83 We recently showed that paracrine signaling controlled by keratinocyte Dsg1 also controls
84 melanocyte behavior (Arnette et al., 2019). Dsg1, but not Ecad, is temporarily lost in a dose
85 dependent manner following acute UV radiation (Johnson et al., 2014). Modeling this behavior,
86 genetic interference resulting in acute loss of Dsg1 affects melanocyte pigmentation and
87 dendricity in a manner reminiscent of the tanning response through secretion of a subset of
88 cytokines also known to be generated in keratinocytes stimulated with UV (Arnette et al., 2019).
89 While acute loss of Dsg1 seems to play a protective role in skin by activating the tanning response,
90 long-term loss of keratinocyte Dsg1 promotes behaviors in melanocytes that mimic a malignant
91 phenotype, such as pagetoid movement in 3D organotypic cultures (Arnette et al., 2019). These
92 observations reveal a potential role for loss of keratinocyte Dsg1 in initiating metastatic spread in
93 the primary melanoma niche, specifically in intra-epidermal movement, an understudied
94 phenomenon in melanoma progression.

95 Here, through a combination of analyses of human melanoma tissues and *in vitro*
96 mechanistic studies, we identify a bi-directional communication pathway between keratinocytes
97 and melanoma cells. This communication depends on the melanoma cells' ability to reduce Dsg1
98 expression. Consequent keratinocyte-dependent paracrine stimulation of a neural crest like
99 signature in melanoma cells associates with increased melanoma cell migration. Our data support
100 the idea that melanoma cells reduce Dsg1 by producing paracrine factors that increase activity of

101 the transcription factor Slug and decrease levels of the Dsg1 transcription factor Grainyhead like
102 1 (Grhl1). The relevance of these changes is supported by analysis of human melanoma sections
103 showing that persistent loss of Dsg1, but not Ecad, is associated with local melanoma spread,
104 reduced Grhl1, and increased Slug. Based on these observations, we propose that melanomas
105 hijack normal keratinocyte to melanocyte crosstalk to maintain a pro-tumor environment.

106

107 **Results**

108 **Desmoglein 1 is reduced in melanoma adjacent keratinocytes in human epidermis**

109 To address whether there is an association between Dsg1 loss and melanoma, benign
110 and malignant melanocytic lesions were stained for Dsg1, Ecad in keratinocytes and Melan-A
111 (Mel-A) to mark melanoma cells (Fig. 1A). Quantifying Dsg1 and Ecad border localization and
112 staining intensity revealed that Dsg1 was significantly reduced in the keratinocytes directly
113 adjacent to the Mel-A positive staining cells (melanocytes/melanoma cells) in melanoma samples
114 compared with distant sites or control tissues (Fig. 1B, C). In contrast, keratinocytes adjacent to
115 melanocytes in benign nevi did not show any alteration in Dsg1 levels. Ecad staining remained
116 unchanged in all conditions, demonstrating that the loss of Dsg1 is not solely attributable to a
117 general loss of cell adhesion proteins in melanoma adjacent keratinocytes (Fig. 1C).

118 **Melanoma cells downregulate keratinocyte Dsg1 through paracrine signaling**

119 Comparisons of chronic sun exposed skin and non-sun exposed skin transcriptomes from
120 the Genotype-Tissue Expression (GTEx) database showed no significant change in Dsg1 gene
121 expression levels (Fig. S1). This, combined with our previous finding that Dsg1 levels recover
122 over time after UV exposure (Johnson et al., 2014), suggests that sustained loss of Dsg1 is likely
123 a disease specific phenomenon and not the result of accumulated sun damage. Furthermore,

124 Dsg1 is maintained in keratinocytes distant from lesional melanoma cells. This led us to ask
125 whether keratinocyte Dsg1 is regulated by the adjacent melanoma cells.

126 To address this question, we began with a unidirectional approach using conditioned
127 media from a panel of melanoma cell lines varying in growth phase and mutation status.
128 Differentiated keratinocytes were cultured in conditioned media from control primary melanocytes
129 or melanoma cell lines, and mRNA or protein was collected and assessed by RT-PCR or
130 immunoblot, respectively. The mRNA and protein levels of Dsg1, but not Ecad or Desmoglein 3
131 (Dsg3), another desmosomal cadherin, were decreased in keratinocytes cultured in melanoma
132 but not melanocyte conditioned media (Fig. 2A, B).

133 To address whether melanoma cells reduce keratinocyte Dsg1 expression in a
134 physiologically relevant model of epidermal differentiation, keratinocytes and melanoma cells or
135 melanocytes were co-cultured for 6 or 10 days at an air-medium interface to stimulate keratinocyte
136 stratification and differentiation. Of the lines tested, WM1341D cells formed discrete tumors along
137 the basement membrane that facilitated accurate quantification of Dsg1 levels in the surrounding
138 keratinocytes. In these 3D cultures, keratinocytes adjacent to melanoma cells, but not normal
139 melanocytes, exhibited a significant decrease in Dsg1, but not Ecad, at the cell borders consistent
140 with what was observed in patient melanoma lesions (Fig. 2C, D). These data show that
141 melanoma cells can downregulate Dsg1 transcription and protein in adjacent keratinocytes, and
142 support the idea that a secreted factor is, at least in part, responsible.

143 **Transcriptomic analysis reveals increased activation of keratinocyte Slug and reduced**
144 **keratinocyte differentiation signaling by melanoma cells**

145 While keratinocyte Dsg1 is vital to the formation and maintenance of a functional
146 epidermis, the mechanisms underlying its transcriptional regulation are poorly understood. To
147 determine what pathways were altered in keratinocytes upstream and downstream of Dsg1 loss,

148 we performed mRNA sequencing on keratinocytes that had been treated with melanoma or
149 melanocyte conditioned media. We utilized gene set enrichment analyses (GSEA) to analyze
150 primary keratinocytes treated with melanoma conditioned media from WM1341D or 501mel cells
151 compared to keratinocytes treated with conditioned media from primary melanocytes, using
152 pathway data characterizing keratinocyte differentiation states in neonatal human skin (Fig. S2A-
153 E) (Wang et al., 2020).

154 This analysis revealed a negative enrichment of gene sets characterizing the most
155 differentiated keratinocyte states (granular and spinous) with some positive enrichment of more
156 basal like transcriptional states (Fig. S2D, E). We previously showed that Dsg1 promotes
157 keratinocyte differentiation through suppression of MAPK signaling. Consistent with this,
158 upstream regulator analysis of our gene expression dataset using Ingenuity Pathway Analysis
159 (IPA), predicted a significant increase in activation of MAPK signaling as indicated by increased
160 ERK1/2 activation (Fig. S2F). This prediction is consistent with our previous finding that activation
161 of MAPK signaling occurs downstream of Dsg1 loss to reduce keratinocyte differentiation.

162 The question remained as to what upstream factors stimulated by treatment with
163 melanoma conditioned media might regulate Dsg1 and the associated differentiation pathways.
164 In this regard, another predicted upstream regulator that emerged was *Snai2* (Slug), which has
165 been associated with stem like properties of epidermal cells, as well as RAC1, which can activate
166 Slug through PAK1 (Thaper et al., 2017; Yao et al., 2020). Slug can directly inhibit the expression
167 of the transcription factor Grhl1, a transcriptional activator of Dsg1 and could mediate the negative
168 enrichment of differentiated keratinocyte gene expression patterns (Mistry et al., 2014;
169 Wilanowski et al., 2008). A potential role for keratinocyte Grhl1 in driving a permissive
170 environment for melanoma progression has never been addressed.

171

172 **Loss of Grhl1 and increased Slug are closely tied with melanoma mediated Dsg1 loss**

173 As Slug/Grhl1 signaling emerged as candidate regulators of Dsg1 in the context of
174 melanoma paracrine signaling, we assessed Grhl1 mRNA and protein levels in keratinocytes
175 treated with melanoma cell conditioned media compared to those treated with melanocyte
176 conditioned media. Grhl1 mRNA and protein were downregulated by melanoma conditioned
177 media but remained unchanged in Dsg1-deficient keratinocytes compared to control indicating
178 that its loss is likely occurring upstream of melanoma induced Dsg1 downregulation (Fig. 3A-D).
179 We also assessed the extent to which Grhl1 is decreased in keratinocytes adjacent to melanoma
180 cells in 3D epidermal equivalent cultures (Fig. 3E). As might be predicted from previous
181 observations that Grhl1 is associated with the epidermal differentiation program, nuclear Grhl1
182 was present in a gradient in control co-cultures, with the most intense nuclear staining present in
183 the superficial, differentiated layers. Whereas Grhl1 was present in the most superficial layers of
184 WM1341D co-cultures, expression was significantly reduced in keratinocytes surrounding tumor
185 nests compared with control (Fig. 3E). Similarly, keratinocytes surrounding melanoma cells in
186 patient samples exhibited reduced Grhl1 staining compared with those surrounding melanocytes
187 in benign nevi (Fig. 3F). Grhl1 levels remained unchanged in Dsg1-deficient cultures compared
188 to control in the 3D culture setting, further indicating that its loss likely occurs upstream of Dsg1
189 downregulation (Fig. 3G). We next examined melanoma regulation of keratinocyte Slug using
190 staining in 3D cultures. Slug exhibited a basal staining pattern in melanocyte containing cultures,
191 as is seen in normal human epidermal tissues. However, nuclear Slug levels were increased in
192 suprabasal keratinocytes adjacent to WM1341D cells (Fig. 3H). Consistent with the decrease in
193 Grhl1 staining in melanoma adjacent keratinocytes, Slug staining was increased in lesional
194 keratinocytes in clinical melanoma tumor sections (Fig. 3I). We found no increase in suprabasal
195 Slug staining in Dsg1 knockdown cultures compared to control, indicating that, like Grhl1, Slug is
196 regulated by melanoma cells upstream of Dsg1 loss (Fig. 3J).

197 Building upon these findings, analysis of a previously published dataset (Mistry et al.,
198 2014) revealed that loss of Slug in primary human keratinocytes led to an increase in Dsg1 and
199 Grhl1 gene expression with no change in Ecad, similar to what we see in keratinocytes in
200 melanoma conditioned media (Fig. S3A). Furthermore, knockout of Slug in keratinocytes using
201 siRNA leads to a concurrent increase in Dsg1 protein levels, supporting the role of Slug as a
202 potential mediator of Dsg1 loss in melanoma associated keratinocytes (Fig. S3B). Together these
203 data support a model whereby melanoma cells mediate an increase in Slug and an accompanying
204 decrease in Grhl1 and its downstream transcriptional target Dsg1 through paracrine signaling to
205 keratinocytes.

206 **Loss of keratinocyte Dsg1 promotes melanoma cell migration *in vitro* and is associated**
207 **with intra-epidermal movement of melanoma cells *in vivo***

208 We next sought to identify the biological consequences of the loss of keratinocyte Dsg1
209 related to malignant behavior in melanoma cells. We performed RNA sequencing of melanoma
210 cells treated with media from control or shDsg1 expressing keratinocytes followed by GSEA using
211 previously published melanoma differentiation state signatures (Tsoi et al., 2018). This analysis
212 revealed an enrichment in a neural crest like signature in melanoma cells treated with Dsg1-
213 deficient keratinocyte media (Fig. 4A). We also observed a negative enrichment of the
214 melanocytic signature, suggesting a general pattern of de-differentiation in these cells. Consistent
215 with this, Gene Ontology (GO) pathway analysis revealed changes in mesoderm formation,
216 negative regulation of cell differentiation, and regulation of EMT pathways, with increased
217 expression of genes that have been linked to neural crest formation (Fig. 4B). Given that these
218 signatures are associated with cell movement and migration, and that loss of keratinocyte Dsg1
219 leads to aberrant, pagetoid movement of melanocytes in 3D epidermal equivalents, we asked
220 whether loss of Dsg1 in keratinocytes in turn promotes melanoma cell migration.

221 To address this question, we cultured melanoma cells in conditioned media from
222 keratinocytes expressing Dsg1 knockdown or control and then performed a trans-well migration
223 assay (Fig. 4C). Melanoma cells cultured in the Dsg1-deficient keratinocyte media showed
224 increased levels of migration while re-introduction of Dsg1 into deficient keratinocytes ameliorated
225 this effect (Fig. 4D, E). These data support the idea that Dsg1 may be important for retaining
226 melanoma cells in the primary tumor niche.

227 To investigate the relationship between keratinocyte Dsg1 and melanoma cell movement
228 *in vivo* we evaluated the extent to which melanoma spread in human patient samples was
229 associated with Dsg1, Ecad, Grhl1 and Slug staining levels in surrounding keratinocytes. Notably,
230 while we did see significant changes in melanoma adjacent Dsg1, Grhl1, and Slug, we observed
231 significant variability in the degree of change of each of these proteins. When we compared the
232 levels of keratinocyte Dsg1 staining to the number of melanoma cells which had begun to move
233 throughout the epidermis, we observed a significant negative correlation between keratinocyte
234 Dsg1 and melanoma epidermal spread (Fig. 5 A, B). Keratinocyte Dsg1 was not correlated with
235 the total number of melanoma cells in the lesions, indicating that the observed change in number
236 of migrating cells are likely not a result of increased cell number (Fig. 5C). Consistent with this,
237 there was no correlation between number of melanoma cells in the niche and the number of cells
238 moving throughout the epidermis.

239 A significant reciprocal association between Grhl1 and local melanoma spread was also
240 observed, while Slug showed a significant positive correlation (Fig. 5 A-C). While there is also
241 variability in keratinocyte Ecad levels in melanoma lesions, we found no significant relationship
242 between Ecad levels and melanoma cell number or melanoma cell movement. These data are
243 consistent with the idea that loss of keratinocyte Dsg1 and its upstream regulator Grhl1 play a
244 role in the initial steps of melanoma cell movement and metastasis. Our data further suggest that

245 paracrine signaling from melanoma cells may control the Dsg1/Grhl1 axis through activation of
246 the repressor of keratinocyte differentiation gene Slug.

247 **Melanoma cells increase ERK1/2 dependent keratinocyte production of CXCL1**
248 **downstream of Dsg1 loss to increase melanoma cell migration**

249 We next investigated how loss of Dsg1 in keratinocytes potentiates melanoma cell
250 movement through paracrine signaling. Our previous work demonstrated that Dsg1-deficient
251 keratinocytes increase secretion of inflammatory cytokines and chemokines, which are known to
252 contribute to the formation and maintenance of the melanoma tumor niche. Chemokines
253 previously identified as increased in the secretome of Dsg1-deficient keratinocytes include the
254 GRO isoforms (CXCL1, CXCL2 and CXCL3), and IL-8 which bind the CXCR1 and 2 receptors,
255 as well as the IL-6 cytokine (Arnette et al., 2019). To address whether keratinocytes grown in
256 melanoma cell conditioned media exhibit increased chemokine expression like that seen with
257 genetic knockdown of Dsg1, we assessed the gene expression levels of chemokines which bind
258 the CXCR1 and CXCR2 receptors, as well as IL-6 in keratinocytes treated with media from
259 WM1341D and 501mel cells. Of the secreted factors tested, we found that melanoma cells drive
260 an increase in CXCL1 expression specifically in keratinocytes (Fig. 6A, Fig. S4).

261 As mentioned above, Upstream Regulator analysis predicted an increase in ERK1/2
262 signaling, which can increase levels of CXCL1 (Cheng et al., 2019; Schweppe et al., 2006). Our
263 previous work showed that genetic interference with Dsg1 results in increased ERK1/2 signaling.
264 Indeed, when active p-ERK/total ERK was measured in keratinocytes grown in melanoma cell
265 conditioned media, a significant increase was observed, like that which occurs in cells with genetic
266 interference of Dsg1 (Fig. 6B). To address whether the observed increase in CXCL1 depended
267 on the ERK1/2 pathway, we treated cells in melanoma conditioned media with the MEK1/2
268 inhibitor U0126. U0126 effectively reduced both ERK1/2 activation as well as CXCL1 gene
269 expression (Fig. 6C, D). Dsg1 levels are not rescued by ERK1/2 inhibition, indicating that

270 melanoma driven ERK1/2 signaling is likely downstream of and mediated by Dsg1 loss as
271 indicated by our transcriptomic analysis.

272 CXCL1 exclusively binds to the CXCR2 receptor in melanoma cells. To confirm the role
273 of CXCL1 in melanoma cell migration we treated melanoma cells with a combination of
274 keratinocyte conditioned media and DMSO or the CXCR2 inhibitor SB225002. When the CXCL1
275 receptor CXCR2 was inhibited in melanoma cells, Dsg1-deficient keratinocytes were no longer
276 able to induce migration, demonstrating a role for specific chemokine signaling in keratinocyte
277 modulation of melanoma cell behavior (Fig. 6E, F). Together these data highlight a novel
278 mechanism of initiation or increase of melanoma cell migration through direct manipulation of
279 tumor niche keratinocytes.

280

281 **Discussion**

282 Melanoma is one of the most aggressive skin cancers, due in part to its propensity to
283 metastasize. The composition of the tumor microenvironment has an undeniably important
284 influence on tumor cell behavior, including metastatic progression. Much of the work done
285 investigating melanoma metastasis has been focused on cells once they have already escaped
286 from the epidermis (Vandyck et al., 2021). Here we examine the underappreciated role of
287 keratinocytes in the initiation (or inhibition) of melanoma cell movement within the primary
288 epidermal niche. Our work establishes a role for the keratinocyte-specific cadherin Dsg1 as a
289 regulator of chemokine signaling whose loss is associated with cell spread in the melanoma tumor
290 niche (Fig. 7). Furthermore, the studies shed light on the understudied mechanisms by which
291 melanoma cells manipulate their epidermal microenvironment to facilitate metastatic progression.

292 Previous work has highlighted the importance of keratinocytes in restricting newly
293 transforming melanocytes to their normal location in the basal epidermis. In particular, the role of

294 cadherins in restricting the movement of melanoma cells has focused on their canonical roles in
295 cell-cell adhesion. For instance, loss of Ecad, which is expressed in both keratinocytes and
296 melanocytes, occurs in progressive fashion in primary/invasive melanomas (Haass et al., 2005).
297 Re-introduction of Ecad into Ecad-deficient melanoma cells inhibited invasion into the dermis of
298 3D reconstructed epidermis through downregulation of invasion receptors MUC18 and β3 integrin
299 (Hsu et al., 2000) and also impairs melanoma cell invasion in response to CXCL12 (Molina-Ortiz
300 et al., 2009). The loss of Ecad in melanoma may also occur in concert with upregulation of pro-
301 migratory N-cadherin, possibly resulting in a cadherin switch similar to that reported for other
302 tumors (Siret et al., 2015). Like Ecad, P-cadherin in the tumor environment promotes keratinocyte-
303 melanoma cell contact. However, in this case the interaction supports the expansion of melanoma
304 cells and progression towards a more aggressive phenotype and poor survival in humans
305 (Mescher et al., 2017). Overall, previous work on cadherins in melanoma progression has focused
306 on the idea of permissive migration due to removal of physical barriers or tumor progression due
307 to cell contact mediated signaling.

308 Here, we provide evidence for a novel paracrine function for the desmosomal cadherin,
309 Dsg1, in shaping the early melanoma microenvironment. While playing an essential role in the
310 physical barrier, Dsg1 has also emerged as a cell autonomous regulator of signaling pathways
311 that complement but do not depend on its physical role in adhesion (Arnette et al., 2019; Getsios
312 et al., 2009; Harmon et al., 2013). Dsg1 loss due to genetic or environmental stimuli revealed a
313 role in controlling differentiation and inflammation (Godsel et al., 2022). The data presented here
314 add to Dsg1 functions, and are consistent with a model whereby its loss in the context of
315 melanoma drives melanoma cell migration. Changes in Dsg1 expression occur before any
316 detectable decrease in Ecad, supporting the idea that these changes occur early in tumor
317 development and that melanoma spread is not an indirect result of loss of this classic cadherin.

318 Consistent with this, melanoma conditioned media is sufficient to mediate a reduction in Dsg1
319 mRNA and protein, in the absence of any significant changes in Ecad expression.

320 Importantly, we have defined for the first time a potential transcriptional regulatory pathway
321 co-opted by melanoma cells to reduce Dsg1 expression through Grhl1 and its upstream
322 transcriptional repressor Slug. While Grhl1 has been shown to regulate epidermal homeostasis
323 by controlling the differentiation program and barrier function (Wilanowski et al., 2008), a role in
324 melanoma development has not been reported. Likewise, Slug has been linked to melanoma cell
325 metastasis but not in the creation of a pro-melanoma keratinocyte compartment (Miao et al., 2021;
326 Shirley et al., 2012). Importantly, while increased Slug likely plays additional roles in shaping the
327 early melanoma tumor environment, genetic targeting of Dsg1 is sufficient to initiate the signaling
328 cascade that stimulates increased melanoma cell movement *in vitro*.

329 Our observation that melanoma cells treated with conditioned media from Dsg1-deficient
330 keratinocytes exhibit a neural crest like signature is consistent with previous studies suggesting
331 malignant melanoma cells hijack the neural crest program to promote plasticity and facilitate
332 invasion and metastasis (Diener and Sommer, 2021; Wessely et al., 2021). We further identify a
333 CXCL1/CXCR2 axis as important for the increase in melanoma cell movement. CXCL1 signaling
334 has been linked to stem cell phenotypes and tumor progression and invasion in other cancers
335 (Tang et al., 2012; Wessely et al., 2021) and CXCR2 introduction into melanoma cells increases
336 cell proliferation, motility and invasion (Singh et al., 2009). CXCR2 may be more prevalent in late-
337 stage melanomas and thus it will be important to explore other potential pathways in the early
338 melanoma niche that could link Dsg1 reduction in keratinocytes to melanoma spread at the
339 earliest stages (Sharma et al., 2010).

340 Finally, here we uncovered novel paracrine regulation of melanoma behavior by the
341 keratinocyte-specific molecule Dsg1. However, this cadherin also controls cell-cell adhesion and
342 the mechanical properties of keratinocytes that along with paracrine signaling could impact

343 melanoma behavior. In the future, understanding how both cell contact mediated and paracrine
344 signaling changes are integrated will be important for acquiring a cohesive understanding of
345 factors shaping the tumor niche. Futhermore, study of how loss of Dsg1 contributes to the
346 plasticity of the tumor cells, whether it stimulates migration of an existing rare population of
347 melanoma cells or lowers the threshold for the emergence of a new population with neural crest
348 features will be important for understanding the molecular mechanisms of communication
349 between these two populations (Emert et al., 2021; Shaffer et al., 2017). As melanoma cells do
350 not acquire new mutations (Shain et al., 2018) once they have left the epidermis, keratinocyte
351 cross talk could be a key shaper of melanoma behavior in the epidermal tumor niche. Changes
352 in melanoma cells caused by a Dsg1-deficient microenvironment maintained over time could be
353 targetable.

354

355 **Materials and Methods**

356 Cell Culture

357 Keratinocytes and melanocytes were isolated from discarded neonatal foreskin provided by the
358 Northwestern University Skin Biology and Diseases Research-Based Center (NUSBDRC) as
359 previously described (Roth-Carter et al., 2022). Keratinocytes were grown in M154 medium
360 supplemented with human keratinocyte growth supplement (Life Technologies), 1,000 x
361 gentamycin/amphotericin B solution (Life Technologies), and 0.07mM $CaCl_2$. Confluent
362 keratinocyte monolayers were differentiated in the media described with addition of 1.2 mM $CaCl_2$.
363 Keratinocytes were transduced with retroviral supernatants produced from Phoenix cells
364 (provided by G. Nolan, Stanford University, Stanford, CA) as previously described (Getsios et al.,
365 2004; Simpson et al., 2010). Melanocytes were cultured in Opti-MEM (Life Technologies)
366 containing 1% penicillin/streptomycin (Corning), 5% fetal bovine serum (FBS) (Sigma-Aldrich), 10

367 ng/ml bFGF (ConnStem Inc), 1 ng/ml heparin (Sigma-Aldrich), 0.1 mM N6, 2'-O-
368 dibutyryladenosine 3:5-cyclic monophosphate (dbcAMP; Sigma-Aldrich), and 0.1 mM 3-isobutyl-
369 1-methyl xanthine (IBMX; Sigma-Aldrich). Melanoma cells were cultured in DMEM containing
370 sodium pyruvate (Life Technologies) with 1% penicillin/streptomycin, 5% FBS (Sigma-Aldrich).
371 WM1341D, WM1366, WM3211 lines were purchased from Rockland Immunochemicals Inc.
372 YUMAC and 501mel lines were kindly gifted by Jaehyuk Choi at Northwestern University. All cell
373 lines were authenticated with DNA (STR) profiling and tested to rule out mycoplasma
374 contamination.

375 Organotypic skin cultures

376 Organotypic cultures were grown as previously described (Arnette et al., 2016; Getsios et al.,
377 2009) with the addition of melanocytes or melanoma cells co-seeded with keratinocytes at a 1:5
378 ratio to mimic the ratio seen in the basal layer of normal skin (Roth-Carter et al., 2022).
379 Organotypic cultures fixed in 10% neutral buffered formalin were embedded in paraffin blocks and
380 cut into 4 μm sections.

381 Preparation of conditioned media

382 Conditioned media from keratinocytes was prepared as previously described (Arnette et al.,
383 2019). Melanocytes or melanoma cells were grown to 70-80% confluence, at which point the
384 media was refreshed and then collected after 72 hours. Conditioned media was added to
385 keratinocytes immediately upon collection.

386 Antibodies and reagents

387 The mouse monoclonal antibodies used were: P124 (anti-Dsg1 extracellular domain; Progen,
388 Heidelberg, Germany), anti-Dsg3 (Progen) 27B2 (anti-Dsg1 cytodomain; Life Technologies), and
389 HMB45 (anti-Melanoma gp100; Thermo Fisher Scientific), total ERK1/2 (Cell Signaling). The
390 rabbit monoclonal antibody EP1576Y (ab52642, anti-S100 beta; Abcam,) was used. Rabbit

391 polyclonal antibodies used were: HECD1 (anti-E-cadherin; Takara), anti-Melan-A (ab15468;
392 Abcam), anti-GAPDH (G9545, glyceraldehyde-3-phosphate dehydrogenase; Sigma-Aldrich),
393 anti-GRHL1 (Thermo Fisher), anti-Slug (Cell Signaling), anti-p-ERK (Cell Signaling), and anti-
394 ERK (Cell Signaling). Secondary antibodies for immunoblotting were goat anti-mouse and goat
395 anti-rabbit (LI-COR). Secondary antibodies for immunofluorescence were goat anti-mouse and
396 goat-anti-rabbit linked to fluorophores of 488, 568, and 647 nm (Alexa Fluor; Life Technologies).
397 DAPI was used to stain nuclei. The MEK1/2 inhibitor (U0126) was purchased from Cell Signaling
398 and used at a 5 μM final concentration. The CXCR2 inhibitor (SB22502) was purchased from
399 Selleck Chemicals and used at a 500 nM final concentration.

400 DNA constructs

401 LZRS-shDsg1 (Dsg1shRNA) and LZRS-Flag Dsg1 were generated as described (Getsios et al.,
402 2009; Simpson et al., 2010). LZRS – NTshRNA was generated as described (Arnette et al., 2016;
403 Getsios et al., 2009). Human SNAI2 siRNA SMART pool was purchased from Dharmacon (5'-
404 UCUCUCCUCUUUCCGGAUA-3', 5'-GCGAUGCCCAGUCUAGAAA-3', 5'-
405 ACAGCGAACUGGACACACA-3', 5'-GAAUGUCUCUCCUGCACAA-3') and transfected as
406 previously described (Arnette et al., 2019).

407 Trans-well migration assay

408 50,000 cells were seeded in 500 μL phenol red-free Opti-MEM in the upper chamber of a 24-well
409 trans-well chamber. DMEM containing 5% FBS was used as a chemoattractant in the lower wells.
410 After 24 hours, inner membranes were scrubbed to remove non-migrated cells. Cells on the outer
411 membranes were fixed in formalin and stained with 0.1% crystal violet. Membranes were excised
412 from the trans-well insert and mounted on glass slides. Migrated cells were visualized by
413 microscopy and counted.

414

415 qPCR

416 Total RNA was extracted from cells using the Quick-RNA miniprep kit (Zymo Research) following
417 the manufacturer's protocol. cDNA was synthesized using 1 µg of RNA using the Superscript III
418 First Strand Synthesis Kit (Thermo Fisher). Quantitative PCR was performed on the QuantStudio
419 3 instrument (Thermo Fisher), using SYBR Green PCR master mix (Thermo Fisher). Relative
420 mRNA levels were calculated using the ΔΔCT method normalized to GAPDH.

421 Immunofluorescence

422 For immunostaining, tissue sections were baked at 60°C overnight and de-paraffinized using
423 xylenes. Samples were then rehydrated through a series of ethanol and PBS washes. Tissues
424 were permeabilized in 0.5% Triton X-100 in PBS. Antigen retrieval was performed by incubation
425 in 0.01 M citrate buffer at 95°C for 15 minutes. Sections were blocked in blocking buffer (1% BSA,
426 2% normal goat serum in PBS) for 60 minutes at 37°C. Samples were then incubated in primary
427 antibody at 4°C overnight, followed by incubation in secondary antibody for 1 hour at 37°C.
428 Images were acquired using an AxioVison Z1 system (Carl Zeiss) with Apotome slide module, an
429 AxioCam MRm digital camera, and either a 20x (0.8 NA Plan-Apochromat) or 40x (1.4 NA, Plan-
430 Apochromat) oil objective. Image analysis was carried out using ImageJ software.

431 Immunoblot

432 Whole cell lysates were collected from confluent monolayers in urea-SDS buffer (8 M urea/1%
433 SDS/60 mM Tris (pH 6.8)/5% ß-mercaptoethanol/10% glycerol) and sonicated. Samples
434 separated by SDS-PAGE were transferred to nitrocellulose, blocked in Odyssey Blocking Buffer
435 (LI-COR Biosciences), and incubated with primary antibodies in blocking buffer overnight at 4°C.
436 After a series of PBS washes, secondary antibodies diluted in blocking buffer at 1:10,000
437 concentration were added to blots for 1 hour at room temperature then washed with a series of

438 PBS washes. Protein bands were imaged using LI-COR Odyssey FC (LI-COR Biosciences).
439 Densitometric analysis was performed on scanned blots using LI-COR Image studio software.

440 RNA sequencing

441 Differentiated keratinocytes were cultured with conditioned media for 48 hours and melanoma
442 cells were cultured with conditioned media from keratinocytes expressing shNT or shDsg1 for 24
443 hours. Total RNA was extracted from cells using the Quick-RNA miniprep kit (Zymo Research)
444 following the manufacturer's protocol. Novogene Co., LTD conducted preparation of the mRNA
445 library and transcriptome sequencing. Analyses were performed in R (version 4.1.2) using
446 Bioconductor libraries and R statistical packages. Differential expression analysis was performed
447 using DESeq2. Genes with p-value < 0.05 and $|\log2(\text{FoldChange})| > 1$ were considered to be
448 differentially expressed. Pathway analysis was performed using Ingenuity Pathway Analysis (IPA)
449 for Upstream Regulators and GSEA.

450 Microarray analysis

451 Microarray analyses of SNAI2 knockdown keratinocytes (GSE55269) were performed in R
452 (version 4.1.2) using Bioconductor libraries and R statistical packages. Affymetrix probe IDs were
453 converted to unique Entrez IDs for analysis, and differential expression comparisons were
454 performed using the Limma package.

455 Statistical analysis

456 Statistical analysis was performed using GraphPad Prism 8.0 software. All experiments were
457 performed at least three times. Measured data were represented as the mean +/- SEM. One-way
458 analysis of variance (ANOVA) or two-tail Student's t-test were applied to compare quantitative
459 data. P-values for each analysis are marked on figures, and the level of statistical significance
460 was defined as *$p<0.05$, ** $p<0.01$, ***$p<0.001$, ****$p<0.0001$.

ACKNOWLEDGMENTS

Research was supported by NIH/NIAMS P30 AR075049 awarded to Northwestern University Skin Biology & Diseases Resource-Based Center. Histology services were provided by the Northwestern University Mouse Histology and Phenotyping Laboratory, which is supported by NCI P30-CA060553, awarded to the Robert H Lurie Comprehensive Cancer Center. This work was supported by NIH/NCI R01 CA228196 with additional support from NIH/NIAMS R01 AR041836, NIH/NIAMS R01 AR043380, a Leo Foundation Grant and the J.L. Mayberry Endowment to KJG. JLP was supported by NIH/NCI T32 CA009560. HEB was supported by NIH/NCI T32 CA080621-14. QRRC was supported by NIH/NCI T32 CA070085. JTS was supported by NIH/NIAMS P30-AR069589.

AUTHOR CONTRIBUTIONS

KJG, HEB and CRA conceived of and designed experiments. HEB, JLK and JLP acquired data. HEB, QRRC and JLP performed imaging and data analysis. CRA and JLJ provided training and technical assistance. PG and JTS provided tissue samples. KJG and HEB wrote the manuscript.

DECLARATION OF INTERESTS

The authors declare no competing interests.

DATA AVAILABILITY

The dataset used during the study is available from the corresponding author upon request.

COMPETING INTERESTS

The authors declare no competing financial interests.

482 **REFERENCES**

483 Arnette, C., J.L. Koetsier, P. Hoover, S. Getsios, and K.J. Green. 2016. In Vitro Model of the
484 Epidermis: Connecting Protein Function to 3D Structure. *Methods Enzymol*. 569:287-308.
485 Arnette, C.R., Q.R. Roth-Carter, J.L. Koetsier, J.A. Broussard, H.E. Burks, K. Cheng, C. Amadi,
486 P. Gerami, J.L. Johnson, and K.J. Green. 2019. Keratinocyte cadherin desmoglein 1
487 controls melanocyte behavior through paracrine signaling. *Pigment Cell Melanoma Res*.
488 Brandner, J.M., and N.K. Haass. 2013. Melanoma's connections to the tumour microenvironment.
489 *Pathology*. 45:443-452.
490 Cheng, Y., X.L. Ma, Y.Q. Wei, and X.W. Wei. 2019. Potential roles and targeted therapy of the
491 CXCLs/CXCR2 axis in cancer and inflammatory diseases. *Biochim Biophys Acta Rev*
492 *Cancer*. 1871:289-312.
493 Diener, J., and L. Sommer. 2021. Reemergence of neural crest stem cell-like states in melanoma
494 during disease progression and treatment. *Stem Cells Transl Med*. 10:522-533.
495 Emert, B.L., C.J. Cote, E.A. Torre, I.P. Dardani, C.L. Jiang, N. Jain, S.M. Shaffer, and A. Raj.
496 2021. Variability within rare cell states enables multiple paths toward drug resistance. *Nat*
497 *Biotechnol*. 39:865-876.
498 Galbo, P.M., Jr., X. Zang, and D. Zheng. 2021. Molecular Features of Cancer-associated
499 Fibroblast Subtypes and their Implication on Cancer Pathogenesis, Prognosis, and
500 Immunotherapy Resistance. *Clin Cancer Res*. 27:2636-2647.
501 Getsios, S., E.V. Amargo, R.L. Dusek, K. Ishii, L. Sheu, L.M. Godsel, and K.J. Green. 2004.
502 Coordinated expression of desmoglein 1 and desmocollin 1 regulates intercellular
503 adhesion. *Differentiation*. 72:419-433.
504 Getsios, S., C.L. Simpson, S. Kojima, R. Harmon, L.J. Sheu, R.L. Dusek, M. Cornwell, and K.J.
505 Green. 2009. Desmoglein 1-dependent suppression of EGFR signaling promotes
506 epidermal differentiation and morphogenesis. *J Cell Biol*. 185:1243-1258.
507 Godsel, L.M., Q.R. Roth-Carter, J.L. Koetsier, L.C. Tsoi, A.L. Huffine, J.A. Broussard, G.N. Fitz,
508 S.M. Lloyd, J. Kweon, H.E. Burks, M. Hegazy, S. Amagai, P.W. Harms, X. Xing, J. Kirma,
509 J.L. Johnson, G. Urciuoli, L.T. Doglio, W.R. Swindell, R. Awatramani, E. Sprecher, X. Bao,
510 E. Cohen-Barak, C. Missero, J.E. Gudjonsson, and K.J. Green. 2022. Translational
511 implications of Th17-skewed inflammation due to genetic deficiency of a cadherin stress
512 sensor. *J Clin Invest*. 132.
513 Golan, T., A.R. Messer, A. Amitai-Lange, Z. Melamed, R. Ohana, R.E. Bell, O. Kapitansky, G.
514 Lerman, S. Greenberger, M. Khaled, N. Amar, J. Albrengues, C. Gaggioli, P. Gonen, Y.
515 Tabach, D. Sprinzak, R. Shalom-Feuerstein, and C. Levy. 2015. Interactions of Melanoma
516 Cells with Distal Keratinocytes Trigger Metastasis via Notch Signaling Inhibition of MITF.
517 *Mol Cell*. 59:664-676.
518 Green, K.J., Q.R. Roth-Carter, C.M. Niessen, and S.A. Nichols. 2020. Tracing the Origins of the
519 Desmosome: A Vertebrate Innovation. *Curr Biol*. 30:R535-R543.
520 Haass, N.K., K.S. Smalley, L. Li, and M. Herlyn. 2005. Adhesion, migration and communication
521 in melanocytes and melanoma. *Pigment cell research / sponsored by the European*
522 *Society for Pigment Cell Research and the International Pigment Cell Society*. 18:150-
523 159.
524 Harmon, R.M., C.L. Simpson, J.L. Johnson, J.L. Koetsier, A.D. Dubash, N.A. Najor, O. Sarig, E.
525 Sprecher, and K.J. Green. 2013. Desmoglein-1/Erbin interaction suppresses ERK
526 activation to support epidermal differentiation. *J Clin Invest*. 123:1556-1570.
527 Hegazy, M., A.L. Perl, S.A. Svoboda, and K.J. Green. 2022. Desmosomal Cadherins in Health
528 and Disease. *Annu Rev Pathol*. 17:47-72.
529 Hsu, M.Y., F.E. Meier, M. Nesbit, J.Y. Hsu, P. Van Belle, D.E. Elder, and M. Herlyn. 2000. E-
530 cadherin expression in melanoma cells restores keratinocyte-mediated growth control and

531 down-regulates expression of invasion-related adhesion receptors. *Am J Pathol*.
532 156:1515-1525.
533 Johnson, J.L., J.L. Koetsier, A. Sirico, A.T. Agidi, D. Antonini, C. Missero, and K.J. Green. 2014.
534 The desmosomal protein desmoglein 1 aids recovery of epidermal differentiation after
535 acute UV light exposure. *J Invest Dermatol*. 134:2154-2162.
536 Kalaora, S., A. Nagler, J.A. Wargo, and Y. Samuels. 2022. Mechanisms of immune activation and
537 regulation: lessons from melanoma. *Nat Rev Cancer*. 22:195-207.
538 Kowalczyk, A.P., and K.J. Green. 2013. Structure, function, and regulation of desmosomes. *Prog*
539 *Mol Biol Transl Sci*. 116:95-118.
540 Mescher, M., P. Jeong, S.K. Knapp, M. Rubsam, M. Saynisch, M. Kranen, J. Landsberg, M.
541 Schlaak, C. Mauch, T. Tuting, C.M. Niessen, and S. Iden. 2017. The epidermal polarity
542 protein Par3 is a non-cell autonomous suppressor of malignant melanoma. *J Exp Med*.
543 Miao, Y., W. Zhang, S. Liu, X. Leng, C. Hu, and H. Sun. 2021. HOXC10 promotes growth and
544 migration of melanoma by regulating Slug to activate the YAP/TAZ signaling pathway.
545 *Discov Oncol*. 12:12.
546 Mistry, D.S., Y. Chen, Y. Wang, K. Zhang, and G.L. Sen. 2014. SNAI2 controls the
547 undifferentiated state of human epidermal progenitor cells. *Stem Cells*. 32:3209-3218.
548 Molina-Ortiz, I., R.A. Bartolome, P. Hernandez-Varas, G.P. Colo, and J. Teixido. 2009.
549 Overexpression of E-cadherin on melanoma cells inhibits chemokine-promoted invasion
550 involving p190RhoGAP/p120ctn-dependent inactivation of RhoA. *J Biol Chem*.
551 284:15147-15157.
552 Polivka, L., S. Hadj-Rabia, E. Bal, S. Leclerc-Mercier, M. Madrange, Y. Hamel, D. Bonnet, S.
553 Mallet, H. Lepidi, C. Ovaert, P. Barbet, C. Dupont, B. Neven, A. Munnich, L.M. Godsel, F.
554 Campeotto, R. Weil, E. Laplantine, S. Marchetto, J.P. Borg, W.I. Weis, J.L. Casanova, A.
555 Puel, K.J. Green, C. Bodemer, and A. Smahi. 2018. Epithelial barrier dysfunction in
556 desmoglein-1 deficiency. *J Allergy Clin Immunol*. 142:702-706 e707.
557 Roth-Carter, Q.R., J.L. Koetsier, J.A. Broussard, and K.J. Green. 2022. Organotypic Human Skin
558 Cultures Incorporating Primary Melanocytes. *Curr Protoc*. 2:e536.
559 Samuelov, L., O. Sarig, R.M. Harmon, D. Rapaport, A. Ishida-Yamamoto, O. Isakov, J.L. Koetsier,
560 A. Gat, I. Goldberg, R. Bergman, R. Spiegel, O. Eytan, S. Geller, S. Peleg, N. Shomron,
561 C.S. Goh, N.J. Wilson, F.J. Smith, E. Pohler, M.A. Simpson, W.H. McLean, A.D. Irvine, M.
562 Horowitz, J.A. McGrath, K.J. Green, and E. Sprecher. 2013. Desmoglein 1 deficiency
563 results in severe dermatitis, multiple allergies and metabolic wasting. *Nat Genet*. 45:1244-
564 1248.
565 Schweppe, R.E., T.H. Cheung, and N.G. Ahn. 2006. Global gene expression analysis of ERK5
566 and ERK1/2 signaling reveals a role for HIF-1 in ERK5-mediated responses. *J Biol Chem*.
567 281:20993-21003.
568 Shaffer, S.M., M.C. Dunagin, S.R. Torborg, E.A. Torre, B. Emert, C. Krepler, M. Beqiri, K.
569 Sproesser, P.A. Brafford, M. Xiao, E. Eggan, I.N. Anastopoulos, C.A. Vargas-Garcia, A.
570 Singh, K.L. Nathanson, M. Herlyn, and A. Raj. 2017. Rare cell variability and drug-induced
571 reprogramming as a mode of cancer drug resistance. *Nature*. 546:431-435.
572 Shain, A.H., N.M. Joseph, R. Yu, J. Benhamida, S. Liu, T. Prow, B. Ruben, J. North, L. Pincus, I.
573 Yeh, R. Judson, and B.C. Bastian. 2018. Genomic and Transcriptomic Analysis Reveals
574 Incremental Disruption of Key Signaling Pathways during Melanoma Evolution. *Cancer*
575 *Cell*. 34:45-55 e44.
576 Sharma, B., S. Singh, M.L. Varney, and R.K. Singh. 2010. Targeting CXCR1/CXCR2 receptor
577 antagonism in malignant melanoma. *Expert Opin Ther Targets*. 14:435-442.
578 Shirley, S.H., V.R. Greene, L.M. Duncan, C.A. Torres Cabala, E.A. Grimm, and D.F. Kusewitt.
579 2012. Slug expression during melanoma progression. *Am J Pathol*. 180:2479-2489.
580 Simpson, C.L., S. Kojima, and S. Getsios. 2010. RNA interference in keratinocytes and an
581 organotypic model of human epidermis. *Methods Mol Biol*. 585:127-146.

582 Singh, S., K.C. Nannuru, A. Sadanandam, M.L. Varney, and R.K. Singh. 2009. CXCR1 and
583 CXCR2 enhances human melanoma tumourigenesis, growth and invasion. *Br J Cancer*.
584 100:1638-1646.
585 Siret, C., C. Terciolo, A. Dobric, M.C. Habib, S. Germain, R. Bonnier, D. Lombardo, V. Rigot, and
586 F. Andre. 2015. Interplay between cadherins and alpha2beta1 integrin differentially
587 regulates melanoma cell invasion. *Br J Cancer*. 113:1445-1453.
588 Tang, K.H., S. Ma, T.K. Lee, Y.P. Chan, P.S. Kwan, C.M. Tong, I.O. Ng, K. Man, K.F. To, P.B.
589 Lai, C.M. Lo, X.Y. Guan, and K.W. Chan. 2012. CD133(+) liver tumor-initiating cells
590 promote tumor angiogenesis, growth, and self-renewal through neurotensin/interleukin-
591 8/CXCL1 signaling. *Hepatology*. 55:807-820.
592 Thaper, D., S. Vahid, K.M. Nip, I. Moskalev, X. Shan, S. Frees, M.E. Roberts, K. Ketola, K.W.
593 Harder, C. Gregory-Evans, J.L. Bishop, and A. Zoubeidi. 2017. Targeting Lyn regulates
594 Snail family shuttling and inhibits metastasis. *Oncogene*. 36:3964-3975.
595 Tsoi, J., L. Robert, K. Paraiso, C. Galvan, K.M. Sheu, J. Lay, D.J.L. Wong, M. Atefi, R. Shirazi, X.
596 Wang, D. Braas, C.S. Grasso, N. Palaskas, A. Ribas, and T.G. Graeber. 2018. Multi-stage
597 Differentiation Defines Melanoma Subtypes with Differential Vulnerability to Drug-Induced
598 Iron-Dependent Oxidative Stress. *Cancer Cell*. 33:890-904 e895.
599 Upadhyay, P.R., T. Ho, and Z.A. Abdel-Malek. 2021. Participation of keratinocyte- and fibroblast-
600 derived factors in melanocyte homeostasis, the response to UV, and pigmentary
601 disorders. *Pigment Cell Melanoma Res*. 34:762-776.
602 Vandyck, H.H., L.M. Hillen, F.M. Bosisio, J. van den Oord, A. Zur Hausen, and V.
603 Winnepenninckx. 2021. Rethinking the biology of metastatic melanoma: a holistic
604 approach. *Cancer Metastasis Rev*. 40:603-624.
605 Villanueva, J., and M. Herlyn. 2008. Melanoma and the tumor microenvironment. *Curr Oncol Rep*.
606 10:439-446.
607 Wang, J.X., M. Fukunaga-Kalabis, and M. Herlyn. 2016. Crosstalk in skin: melanocytes,
608 keratinocytes, stem cells, and melanoma. *J Cell Commun Signal*. 10:191-196.
609 Wang, S., M.L. Drummond, C.F. Guerrero-Juarez, E. Tarapore, A.L. MacLean, A.R. Stabell, S.C.
610 Wu, G. Gutierrez, B.T. That, C.A. Benavente, Q. Nie, and S.X. Atwood. 2020. Single cell
611 transcriptomics of human epidermis identifies basal stem cell transition states. *Nat*
612 *Commun*. 11:4239.
613 Wessely, A., T. Steeb, C. Berking, and M.V. Heppt. 2021. How Neural Crest Transcription Factors
614 Contribute to Melanoma Heterogeneity, Cellular Plasticity, and Treatment Resistance. *Int*
615 *J Mol Sci*. 22.
616 Wilanowski, T., J. Caddy, S.B. Ting, N.R. Hislop, L. Cerruti, A. Auden, L.L. Zhao, S. Asquith, S.
617 Ellis, R. Sinclair, J.M. Cunningham, and S.M. Jane. 2008. Perturbed desmosomal
618 cadherin expression in grainy head-like 1-null mice. *Embo J*. 27:886-897.
619 Yao, D., C. Li, M.S.R. Rajoka, Z. He, J. Huang, J. Wang, and J. Zhang. 2020. P21-Activated
620 Kinase 1: Emerging biological functions and potential therapeutic targets in Cancer.
621 *Theranostics*. 10:9741-9766.
622 Yardman-Frank, J.M., and D.E. Fisher. 2021. Skin pigmentation and its control: From ultraviolet
623 radiation to stem cells. *Exp Dermatol*. 30:560-571.

624

625

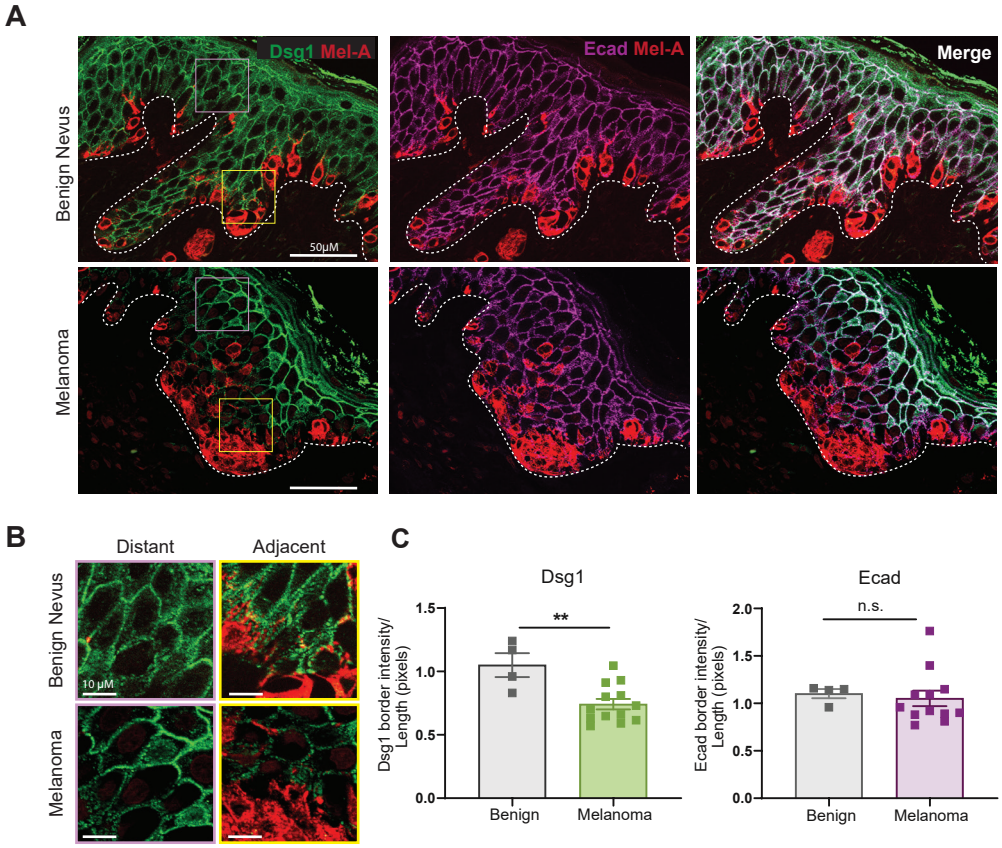

Figure 1: Desmoglein 1 is reduced in melanoma adjacent keratinocytes in human epidermis. A) Paraffin-embedded sections of benign nevi and primary stage melanoma were co-stained for desmoglein 1 (Dsg1) or Ecad and Mel-A to highlight cadherins at cell-cell interfaces of keratinocytes surrounding pigmented cells. Dashed line indicates basement membrane. B) Both distant (2-4 cells away) and proximal keratinocytes were examined for cadherin staining for quantification. C) Pixel intensities were determined for 4 benign and 12 melanoma samples and the ratio of distant to proximal intensities plotted. A significant decrease in Dsg1, but not Ecad, intensity proximal to the melanoma lesions was observed. Mean +/- SEM depicted. **$p < 0.01$. Student's t-test.

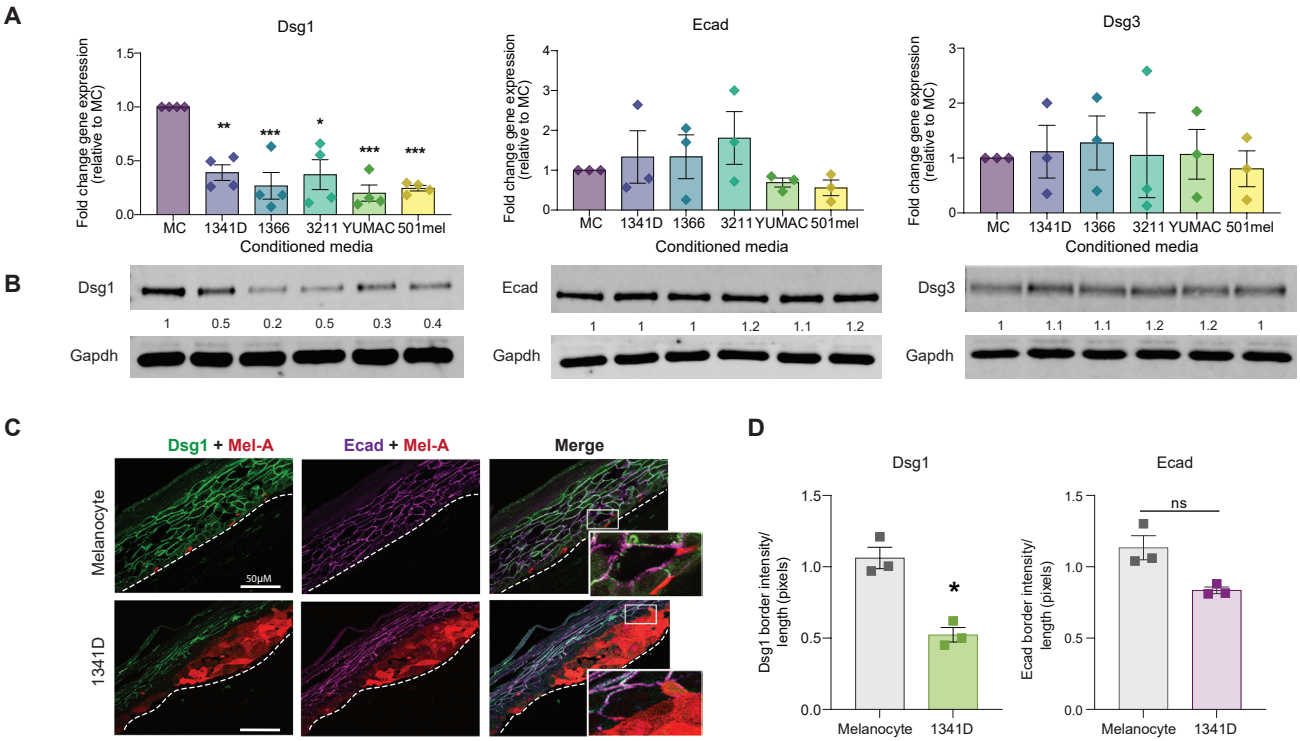

Figure 2: Melanoma cells downregulate keratinocyte Dsg1 through paracrine signaling. Primary human keratinocytes were treated for 24 hours with conditioned media from melanocytes (MC) or the melanoma cell lines 1341D, 1366, 3211, YUMAC and 501mel and RNA or protein was collected. RT-PCR (A) and Western blots (B) were performed for Dsg1, Ecad and Dsg3. Significantly lower mRNA and protein expression of Dsg1, but not Ecad or Dsg3 was observed. n=3. Mean +/- SEM depicted. *p<0.05; **p<0.01; ***p<0.001. One-way ANOVA. C) Melanocytes or 1341D melanoma cells were seeded with normal primary keratinocytes and grown as 3D organotypic raft co-cultures for up to 10 days. Paraffin sections were co-stained for Dsg1 or Ecad and Mel-A. Dashed line indicates basement membrane. D) Pixel intensities were determined and the ratio of distant to proximal intensities plotted. A significant decrease in Dsg1, but not Ecad, intensity proximal to the 1341D lesions was observed. Mean +/- SEM depicted. n=3. *p<0.05, Student's t-test.

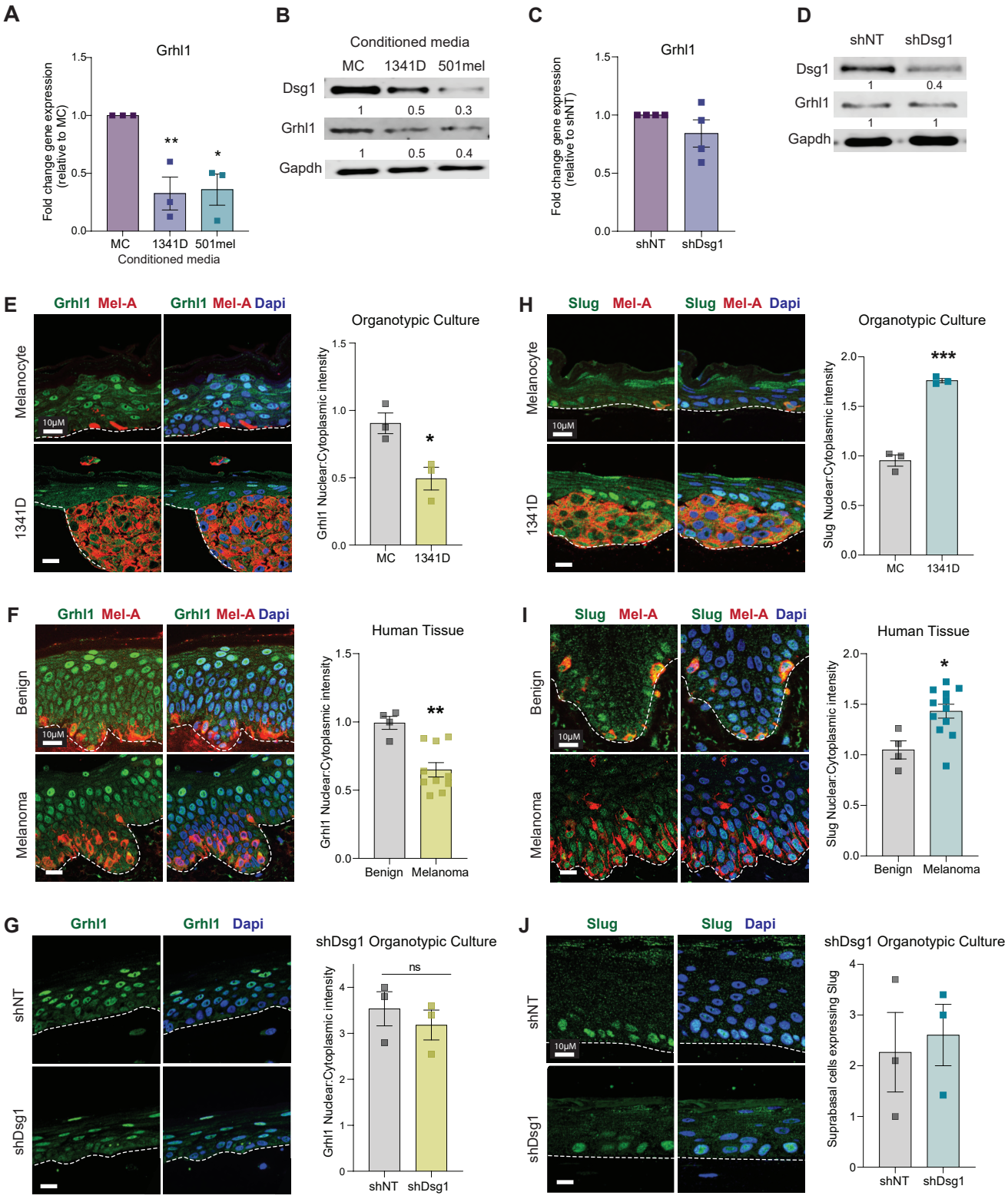
A
Grhl1
Fold change gene expression (relative to MC)
1.5
1.0
0.5
0.0
**
*
MC
1341D
501mel
Conditioned media
B
Conditioned media
MC
1341D
501mel
Dsg1
1
0.5
0.3
Grhl1
1
0.5
0.4
Gapdh
C
Grhl1
Fold change gene expression (relative to shNT)
1.5
1.0
0.5
0.0
shNT
shDsg1
D
shNT
shDsg1
Dsg1
1
0.4
Grhl1
1
1
Gapdh
E
Grhl1 Mel-A
Grhl1 Mel-A Dapi
Melanocyte
1341D
10μM
Organotypic Culture
Grhl1 Nuclear:Cytoplasmic intensity
1.5
1.0
0.5
0.0
*
MC
1341D
H
Slug Mel-A
Slug Mel-A Dapi
Melanocyte
1341D
10μM
Organotypic Culture
Slug Nuclear:Cytoplasmic intensity
2.0
1.5
1.0
0.5
0.0
***
MC
1341D
F
Grhl1 Mel-A
Grhl1 Mel-A Dapi
Benign
Melanoma
10μM
Human Tissue
Grhl1 Nuclear:Cytoplasmic intensity
1.5
1.0
0.5
0.0
**
Benign
Melanoma
I
Slug Mel-A
Slug Mel-A Dapi
Benign
Melanoma
10μM
Human Tissue
Slug Nuclear:Cytoplasmic intensity
2.0
1.5
1.0
0.5
0.0
*
Benign
Melanoma
G
Grhl1
Grhl1 Dapi
shNT
shDsg1
shDsg1 Organotypic Culture
Grhl1 Nuclear:Cytoplasmic intensity
4
3
2
1
0
ns
shNT
shDsg1
J
Slug
Slug Dapi
shNT
shDsg1
10μM
shDsg1 Organotypic Culture
Suprabasal cells expressing Slug
4
3
2
1
0
shNT
shDsg1

Figure 3: Loss of Grhl1 is associated with melanoma mediated Dsg1 loss. A-B) Primary human keratinocytes were treated for 24 hours with conditioned media from melanocytes (MC) or the melanoma cell lines 1341D and 501mel and RNA or protein was collected. RT-PCR and Western blots were performed for Grhl1. Significantly lower mRNA and protein expression of Grhl1 was observed in the keratinocytes treated with melanoma conditioned media when compared with melanocyte control conditioned media. RNA levels and quantification for blots represent average fold change. Mean +/- SEM depicted. n=3. *p<0.05, **p<0.01, *** p <0.001. one-way ANOVA. C-D) Retroviral transduction of shNT (non-targeting control) or shDsg1 knockdown vectors was performed in primary human keratinocytes and RNA or protein collected for RT-PCR and western blot validation of knockdown. No significant difference in Grhl1 mRNA expression or protein level was observed in response to Dsg1 knockdown. E) Melanocytes or 1341D melanoma cells were seeded with normal primary keratinocytes and grown as 3D organotypic raft co-cultures for 6 days. Paraffin sections were co-stained for Grhl1 and Mel-A. Pixel intensities were determined and the ratio of distant to proximal intensities plotted. A significant decrease in Grhl1 intensity proximal to the 1341D lesions was observed. Mean +/- SEM *p<0.05. Student's t-test. F) Paraffin-embedded sections of benign nevi and melanomas were co-stained for Grhl1 and Mel-A and nuclear and cytoplasmic pixel intensities measured in cells proximal to Mel-A stained cells and plotted as nuclear/cytoplasmic ratios. A significant decrease in keratinocyte Grhl1 intensity was observed in keratinocytes adjacent to melanoma compared with those in benign nevi. Mean +/- SEM depicted. n>3. **p<0.01. Student's t-test. G) Similarly, 3D organotypic raft cultures comprised of shNT or shDsg1 expressing keratinocytes were grown for 6 days and stained for Grhl1. Nuclear to cytoplasmic staining intensity of Grhl1 was not statistically different between the two cultures. Mean +/- SEM depicted. n=3, Student's t-test. H) Melanocytes or 1341D melanoma cells were seeded with primary keratinocytes and grown as 3D organotypic raft co-cultures for 6 days. Paraffin sections were co-stained for Slug and Mel-A. Pixel intensities were determined and the ratio of distant to proximal intensities plotted. A significant increase in Slug intensity proximal to the 1341D lesions was observed. +/- SEM ***p<0.001. Student's t-test. I) Paraffin-embedded sections of benign nevi and melanomas were co-stained for Slug and Mel-A. Nuclear and cytoplasmic pixel intensities were measured in cells proximal to Mel-A stained cells and the nuclear/cytoplasmic ratios were plotted. A significant increase in keratinocyte Slug intensity was observed in keratinocytes adjacent to melanoma compared with those in benign nevi. Mean +/- SEM depicted. n>3. *p<0.05. Student's t-test J) 3D organotypic raft cultures comprised of shNT or shDsg1 expressing keratinocytes were grown for 6 days and stained for Slug and the number of suprabasal Slug expressing cells was counted. The number of suprabasal Slug expressing cells was not different between the two cultures. n=3. Student's t-test.

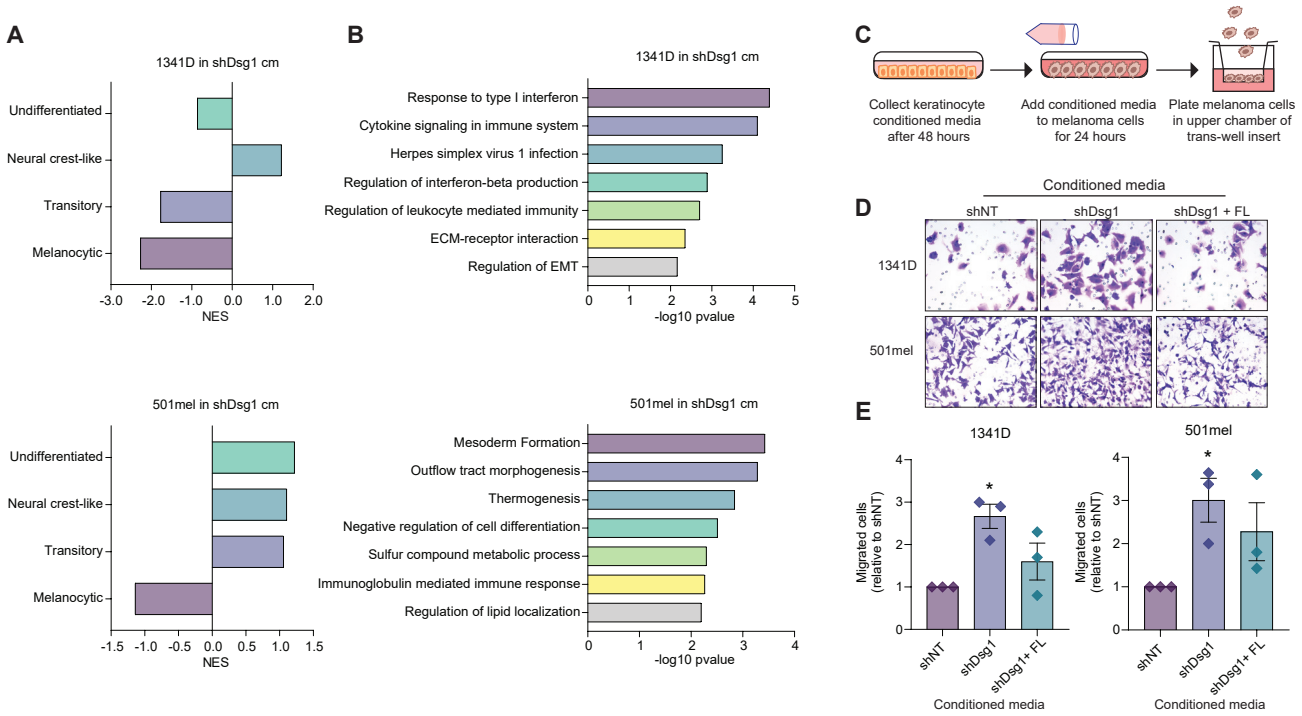

Figure 4: Loss of keratinocyte Dsg1 drives melanoma cell migration. Melanoma cells were cultured for 24 hours in conditioned media from keratinocytes transduced with shNT or shDsg1 knockdown vectors and collected for RNA-sequencing. A, B) Gene set enrichment analysis (GSEA) comparing differentially expressed gene sets to published signatures of melanoma signaling and differentiation. Normalized enrichment score (NES). B) Top Gene Ontology (GO) Biological Process terms overrepresented in genes upregulated by shDsg1 keratinocyte conditioned media. C) Schematic of trans-well migration assay. Melanoma cells were cultured in conditioned media from shNT expressing keratinocytes or shDsg1 expressing keratinocytes for 24 hours. 50,000 cells were then seeded in serum free media in the upper chamber of a trans-well insert (8 μM pore size). Lower wells contained DMEM supplemented with 5% fetal bovine serum (FBS). D, E) After 24 h, migrated cells were fixed and stained for visualization. Bars represent normalized migration compared with shNT control conditioned media. Mean +/- SEM depicted. n=3 *$p < 0.05$ Student's t-test.

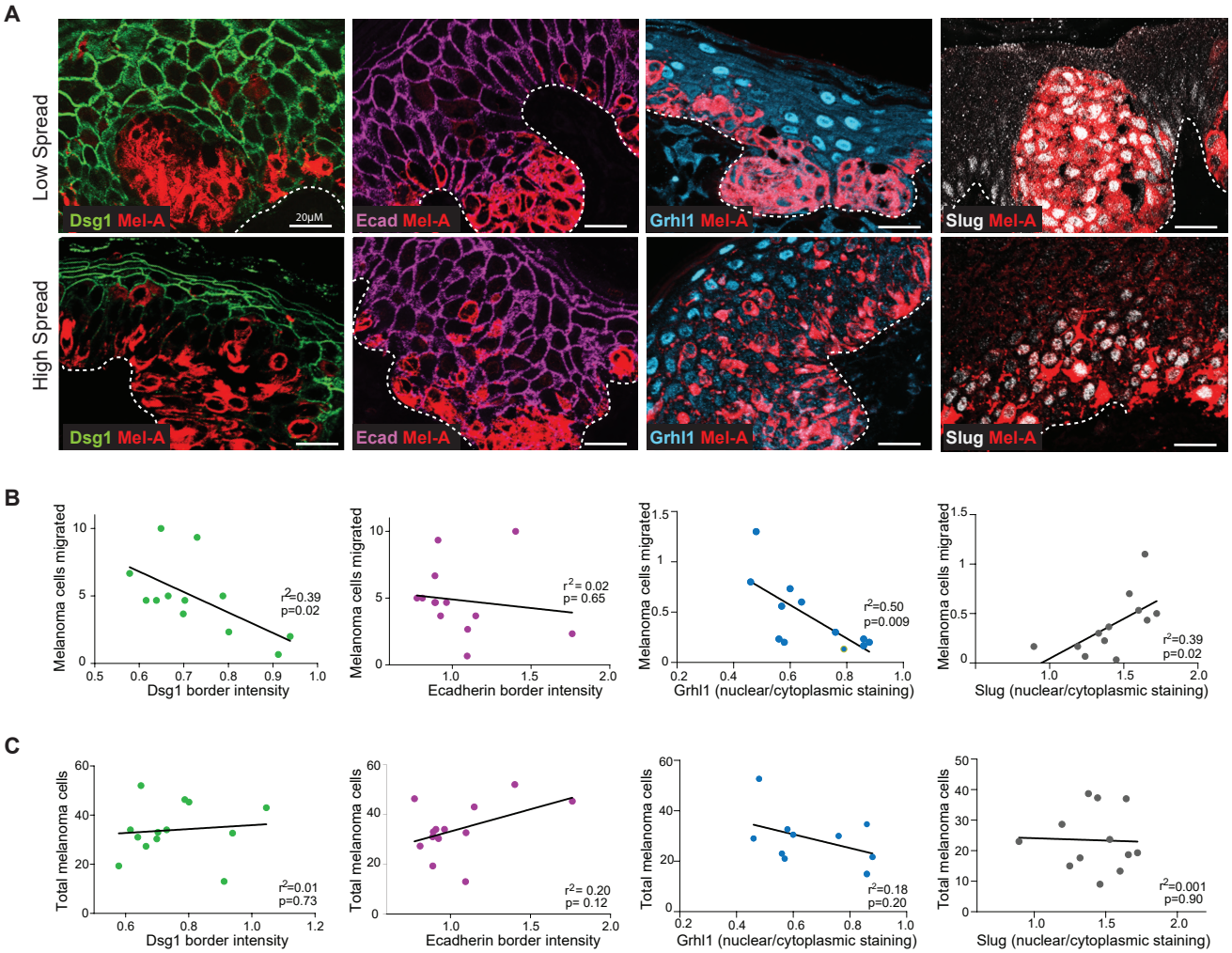

Figure 5. Dsg1 and its regulators are associated with epidermal spread of melanoma cells *in vivo*. Paraffin-embedded sections of melanoma lesions were stained for Dsg1, Grhl1, Slug, or Ecad and Mel-A. The number of individual melanoma cells spreading away from the basal layer, (B) as well as the total number of melanoma cells in each section (C) were counted, and then correlated to the staining intensity of Dsg1, Grhl1, Slug and Ecad. n>10. Simple linear regression.

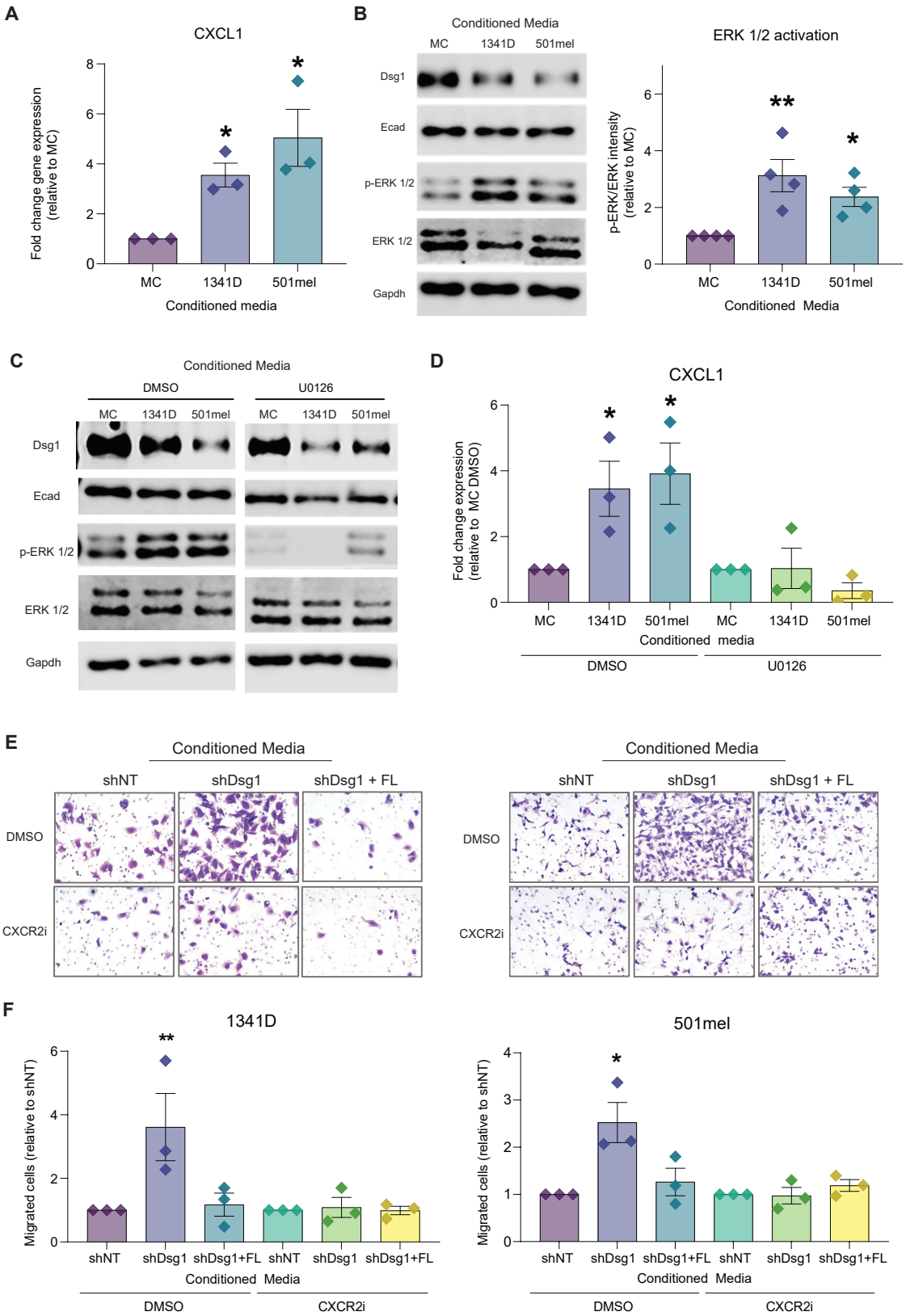
A
CXCL1
Fold change gene expression (relative to MC)
MC
1341D
501mel
Conditioned media
B
Conditioned Media
MC
1341D
501mel
Dsg1
Ecad
p-ERK 1/2
ERK 1/2
Gapdh
ERK 1/2 activation
p-ERK/ERK intensity (relative to MC)
Conditioned Media
C
Conditioned Media
DMSO
U0126
D
CXCL1
Fold change expression (relative to MC DMSO)
Conditioned media
E
Conditioned Media
shNT
shDsg1
shDsg1 + FL
DMSO
CXCR2i
F
1341D
501mel
Migrated cells (relative to shNT)
shDsg1+FL
Conditioned Media

Figure 6. Melanoma induced loss of keratinocyte Dsg1 drives ERK1/2 dependent pro-migratory CXCL1 production. A) Primary human keratinocytes were treated for 48 hours with conditioned media from melanocytes (MC) or the melanoma cell lines 1341D and 501mel and RNA or protein was collected. RT-PCR was performed for CXCL1 expression. Mean +/- SEM depicted. n=3. *p< 0.05, One-way ANOVA. B) Western blot was performed for Dsg1, Ecad, ERK1/2 and phospho-ERK1/2 Mean +/- SEM depicted. n=4, *p< 0.05 **p<0.01. One-way ANOVA. Increased ERK1/2 phosphorylation was observed in keratinocytes treated with melanoma conditioned media. C) Primary human keratinocytes were treated with melanocyte or melanoma conditioned media with either DMSO or 5 μM U0126 (MEK1/2 inhibitor). Western blot was performed to confirm a decrease in ERK1/2 phosphorylation in U0126 treated cells. n=3. D) CXCL1 gene expression was no longer increased in keratinocytes treated with melanoma conditioned media in the presence of U0126 n=3. *p< 0.05. One-way ANOVA. E, F) Melanoma cells were treated with conditioned media from shNT, shDsg1, or shDsg1 plus a full length (FL) wild-type Dsg1 rescue expressing keratinocytes for 24 hours in the presence of DMSO or the CXCR2 inhibitor (500 nM SB22502) then plated for trans-well migration and collected after 24 hours. Loss of keratinocyte Dsg1 no longer increased melanoma cell migration when the CXCL1 receptor, CXCR2, was inhibited Mean +/- SEM depicted. n=3 *p < 0.05 **p< 0.01. One-way ANOVA.

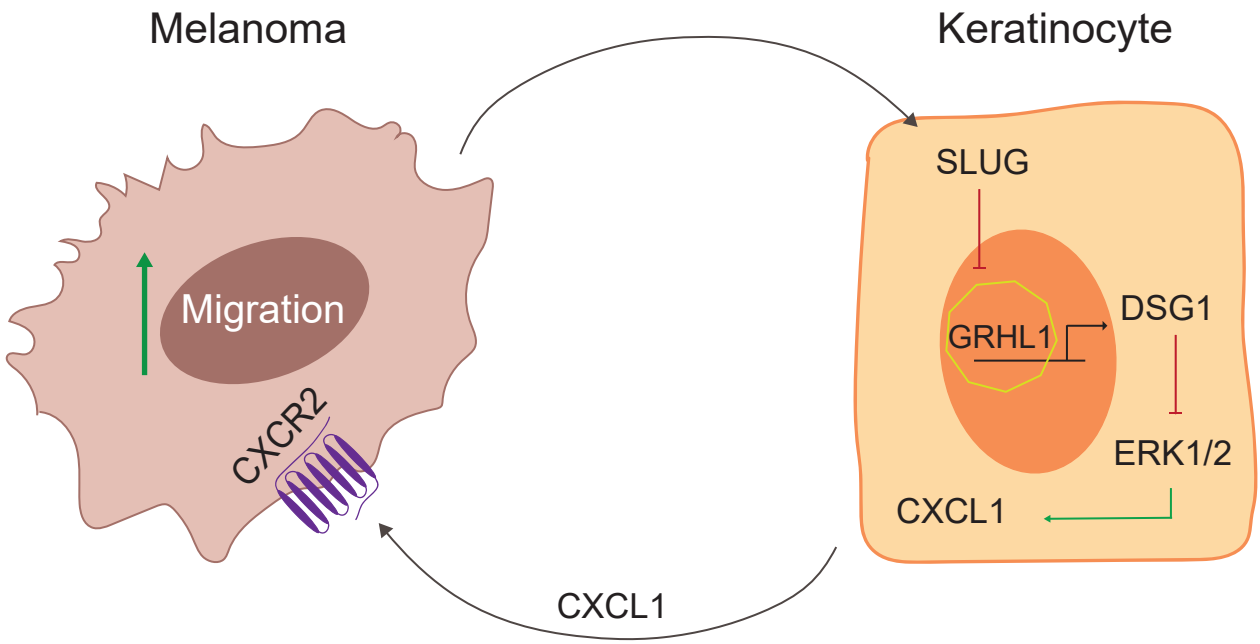

Figure 7. Model: Bi-directional paracrine signaling between melanoma cells and keratinocytes potentiates melanoma cell movement. Our data support a model whereby factors secreted from melanoma cells activate keratinocyte Slug, which in turn decreases Grhl1, a transcriptional activator of Dsg1. The consequent loss of Dsg1 activates ERK1/2 to increase keratinocyte CXCL1 production, which in turn promotes melanoma cell migration through activation of CXCR2.